SPE 152754

Building Trust in History Matching: The Role of Multidimensional Projection

Yasin Hajizadeh, SPE, Elisa Portes dos Santos Amorim, Mario Costa Sousa, Department of Computer Science, University of Calgary

This paper was prepared for presentation at the EAGE Annual Conference & Exhibition incorporating SPE Europec held in Copenhagen, Denmark, 4–7 June 2012.

Abstract

Assisted history matching frameworks powered by stochastic population-based sampling algorithms have been a popular choice for real-life reservoir management problems for the past decade. These methods provide an ensemble of history-matched models which can be used to quantify the uncertainty of future field performance. As a critique, population-based algorithms are generally considered black-boxes with little knowledge of their performance during history matching. In most cases, the misfit value is used as the only criteria to monitor the sampling algorithms and assess their quality.

This paper applies three recently developed multidimensional projection schemes as a novel interactive, exploratory visualization tool for gaining insights to the sampling performance of population-based algorithms and comparing multiple runs in history matching. We use Least Square Projection (LSP), Projection by Clustering (ProjClus) and Principle Component Analysis (PCA) to examine the relationship between exploration of search space and the uncertainty in predictions of reservoir production. These projection techniques provide a mapping of the high dimensional search space into a 2D space by trying to maintain the distance relationships between sampled points. The application of multidimensional projection is illustrated for history matching of the benchmark PUNQ-S3 model using ant colony, differential evolution, particle swarm and the neighbourhood algorithms.

We conclude that multi-dimensional projection algorithms are valuable diagnostic tools that should accompany assisted history matching workflows in order to evaluate their performance and compare ensembles of history-matched models. Using the projection tools, we show that misfit value - as an indicator of match quality - is not the only important factor in making reliable predictions. We demonstrate that exploration of the search space is also a critical element in the uncertainty quantification workflow which can be monitored with multidimensional projection schemes.

Introduction

History matching is a process where the reservoir simulation model is conditioned to the available field data. It aims to tune the model in order to be consistent with the field performance. A simulation model which can capture the past life of a reservoir is more likely to make accurate predictions. History matching is an ill-posed inverse problem with non-unique solutions. Multiple realizations of the reservoir may give equally good matches to available data. Over the years our industry has moved from “in data we trust” to “in uncertainty we trust”. One of the main concerns in reservoir engineering studies is to get reliable production forecasts to make optimal management decisions both from technical and economical viewpoints.The ultimate goal of a history matching study is to have calibrated reservoir models with high prediction capability.

Population-based optimization (sampling) algorithms have recently enjoyed growing popularity for tackling history matching problems. These systems work with a group of individuals that cooperate and communicate to accomplish a task that is normally beyond the capabilities of each individual. These individuals are deployed to search for multiple combinations of uncertain parameters of the simulation model that can give a good match to available field data. This is achieved by minimizing an objective function value (misfit) defined for various targets such as pressures and rates in both well and field levels. Novel adaptive stochastic methods also provide the opportunity to balance exploration and exploitation while searching for optimal solutions. Exploration refers to the search of different areas in the parameter space while exploitation is

the refinement of the previously visited regions to find better answers. Genetic algorithm [Romero et al. 2000], evolutionary strategy [Schulze-Riegert et al. 2001], neighbourhood algorithm [Christie et al. 2002], ant colony optimization [Hajizadeh et al. 2009], differential evolution [Hajizadeh et al. 2010], particle swarm optimization [Mohamed et al. 2010], estimation of distribution algorithms [Abdollahzadeh et al. 2011] and hybrids of these methods are all examples of population-based sampling techniques that have been applied to history matching problems. The success of these algorithms has made them the primary choice for most of the current commercial assisted history matching packages.

Population-based methods in general can also efficiently address the second aspect of any history matching study - uncertainty of the predictions. The uncertainty quantification is (usually) performed through combining a form of Monte Carlo technique with a proxy modeling algorithm (based on the samples obtained in history matching phase). The proxy modeling is required to eliminate the need for running a large number of full simulations in Monte Carlo techniques.

One of the main concerns raised by people involved in history matching studies is that they have no or little information regarding the performance of sampling algorithms at the heart of their assisted history matching frameworks. Within this context, misfit value is usually the only choice for comparing different algorithms and ensembles of history-matched models. However, previous studies suggested that a good fitting model with a low misfit value is not necessarily a good predictor [Tavasolli et al. 2004].

In this paper, we propose a novel approach to visualize the sampling algorithms in an assisted history matching workflow which gives additional information about the performance of these algorithms. We discuss the relationship between the sampling performance of population-based algorithms and the uncertainty estimates obtained for future reservoir performance. The tools presented in this study can also help to decide the right balance between exploration and exploitation of search space in assisted history matching.

Multi-Dimensional Projection

In real-life history matching cases, we usually deal with a high-dimensional problem with many unknown variables being adjusted during the process. Handling the large number of unknowns is not only difficult from computational aspects of sampling in high dimensional spaces – i.e. curse of dimensionality [Bengtsson et al. 2008], but also poses a great challenge in visualizing the results. The challenge comes from the limited ability of the user's visual perception and the number of dimensions that can be visualized. Considering each uncertain variable in history matching as a dimension, models in an assisted history matching framework using a sampling (optimization) algorithm can be viewed as vectors placed in a *m*-dimensional space. Multidimensional projection provides a way to overcome this challenge by reducing the dimensionality of data and projecting the resulted points into a lower dimensional space (1D, 2D, 3D). This mapping aims at maintaining the distance relationship between the data points in the original space. However one should bear in mind that information loss during the projection process is unavoidable and the ultimate goal of the projection algorithms is to minimize such losses.

Latest developments in the field of information visualization and novel multidimensional data visualization techniques can be a significant improvement to our understanding of the history matching process and the results we obtain. We aim to recognize the patterns in our results, understand the performance of the sampling algorithm and see how the algorithm has navigated the search space. Also, as stated by Buja et al. [2009], exploratory plots can take the role of test statistics and human cognition the role of statistical tests. This framework helps to furnish the visual data discovery with a tool to drive confirmatory inference on dependency and importance of various parameters in a modeling study.

In the next section, we briefly introduce three multidimensional projection techniques (Least Square Projection, Projection by Clustering and Principle Component Analysis) that are implemented in the Projection Explorer (PEx) tool [Paulovich et al. 2007] - publicly available from (http://infoserver.lcad.icmc.usp.br/infovis2/PEx).

Least Square Projection (LSP)

The Least Square Projection (LSP) technique was introduced by Paulovich et al. [2006] and is one of the most robust amongst projection methods, both in terms of computational cost and solution preciseness. The core of the method consists on solving a system of linear equations, whose solution is the final projection of the given dataset. The assembly of such linear system is acquired through two main steps. In the first step, one equation is written for each instance, describing its final projected position as a dependency of it high-dimensional neighbors' final positions. The idea is to preserve the original distances as much as possible in the projection process.

Let us consider a set of points $S = \{p_1, p_2, \ldots, p_n\}$ to be a dataset with n instances defined on R^m. Let $V_i = \{p_{i_1}, p_{i_2}, \ldots, p_{i_{ki}}\}$ be a set of k_i points in a neighborhood of a point p_i and $\tilde{p}_i$ be the coordinates of p_i in R^d, where d is the projection target

dimension. We write $\tilde{p}_i$ in terms of the following equation:

$$\tilde{p}_i - \sum_{p_{j \in V_i}} \alpha_{ij}\, \tilde{p}_j = 0, \qquad 0 \le \alpha_{ij} \le 1;\ \sum \alpha_{ij} = 1 \tag{1}$$

where α_{ij} is inversely proportional to the distance between p_i and p_j in the original space. Writing a similar equation to every instance in the dataset gives part of the LSP system,

$$L\tilde{p} = 0 \tag{2}$$

The entries of matrix L are given by:

$$l_{ij} = \begin{cases} 1 & i = j \\ -\alpha_{ij} & p_j \in V_i \\ 0 & otherwise \end{cases} \tag{3}$$

The remaining equations of the system are acquired in a second step, which requires the selection of a subset of instances, called *control points*. An initial position in R^d is assigned to each one of the control points by a *Multidimensional Scaling* method (MDS). Each control point will add a new equation to the system, playing the role of a constraint, since the exact mapping from R^m to R^d is known. Thus, given n_c control points, equation 2 can be rewritten as:

$$\boldsymbol{A\tilde{p} = b} \tag{4}$$

where *A* is a rectangular matrix $(n + nc) \times n$ given by:

$$A = \binom{L}{C},\ c_{ij} = \begin{cases} 1 & p_j\ is\ a\ control\ point \\ 0 & otherwise \end{cases} \tag{5}$$

And **b** is the vector given by:

$$b_i = \begin{cases} 0 & i \le n \\ \tilde{p}_{pci} & n < i \le n + n_c \end{cases} \tag{6}$$

where $\tilde{p}_{pci}$ is one of the cartesian coordinates of the control point p_{ci}. The solution of system (4) is $\tilde{p}$ that minimizes $\|A\tilde{p} - b\|^2$, which gives the final projection of the instances of the dataset.

Projection by Clustering (ProjClus)

The Projection by Clustering (ProjClus) technique was first introduced as an alternative to aid the categorization of text documents [Paulovich and Minghim, 2006]. However, the technique is general enough to handle any kind of high dimensional data.

The technique is very simple and works as follows. Let $X = (p_1, p_2, \ldots, p_n\}$ be a dataset with *n* instances defined on R^m. The goal is to project set *X* to a lower (two) dimensional space (R^2) while preserving their distance relationship given by a specific metric. If we define $d(x_i, x_j)$ a proximity criterion between points in the original space and $\hat{d}(\alpha(x_i,), \alpha(x_j))$ a proximity function in the projected space via the projection function (α), ProjClus aims to approximate the difference between $d(x_i, x_j)$ and $\hat{d}(\alpha(x_i,), \alpha(x_j))$ as close as possible to zero.

ProjClus starts by splitting *X* into $\sqrt{N}$ clusters denoted by $S_1, S_2, \ldots, S_k$ using the bisecting k-means technique. The subsequent step consists of calculating the centroid (*C*) of each cluster, arranging them as a new dataset $C = \{c_1, c_2, \ldots, c_k\}$. Afterwards, each cluster is individually projected to a lower-dimensional space (R^2), as if they were separated datasets, using the Fastmap projection technique [Faloutsos and Lin, 1995]. As the last step, cluster centroids are projected to the 2D space using Fastmap. Finally, the projection of each cluster is repositioned in R^2 according to its relative position to the centroids.

Principle Component Analysis (PCA)

Principle component analysis (PCA) is a class of linear projection techniques that aims to reduce the dimensionality of data

by transforming it into a new set of variables –principles components- that are linear combinations of the original variables. These components are ordered so that the first few of them represent the substantial proportion of the variation in all of the original variables. PCA operates by decomposing the covariance matrix of the data into *m* eigenvectors with *m* eigenvalues and selecting the first *p* eigenvectors with the largest eigenvalues to transform the *m*-dimensional space into a *p*-dimensional space.

According to Hotelling [1933], for a given set of data vectors, the *d* principal axes are those orthonormal axes onto which the variance retained under projection is maximal. PCA uses a linear transformation to form a simplified data set keeping the characteristics of the original data. Assume that *X* is the original data matrix that contains *m* dimensions and *n* observations. In order to achieve the maximum variance, the principle component (*Y*) is written as a linear combination of X defined by coefficients or weights in matrix form:

$$Y = w^T X \tag{7}$$

$$var\,(Y) = var\,(w^T X) = w^T S_w \tag{8}$$

where *S* is the sample covariance matrix of *X*. We choose *w* to maximize $w^T S_w$ while constraining *w* to have unit length. PCA has been widely used for visualization of high dimensional data in various application domains [Yang et al. 2003] [Santos and Brodlie, 2004]. Recently an interactive version of this algorithm is proposed for visualization purposes [Jeong et al. 2009]. For a discussion on challenges of integration between PCA and the visualization process, one can refer to [Muller et al. 2006].

The next section will reexamine the history matching results of the PUNQ-S3 using ant colony, differential evolution, particle swarm and the neighbourhood algorithms, previously reported by Hajizadeh et al. [2011].

History Matching of PUNQ-S3 Reservoir Model

PUNQ-S3 is a synthetic model based on a real-field reservoir in the North Sea operated by Elf Exploration and Production [Boss, 1999]. The PUNQ-S3 has been used widely to compare different history matching and uncertainty quantification workflows [Manceau et al. 2001] [Mantica et al. 2002] [Gao et al. 2007]. As described by Floris et al. [2001], the PUNQ-S3 model has 5 layers with a top depth of 2430 meters. It is bounded by a fault to the east and south and has a relatively strong aquifer on the north and west that provides a pressure support. Six production wells are marked with black dots in figure 1. The PUNQ-S3 model has 19×28×5 grid blocks. The complete data set for this reservoir is available online [PUNQ, 2011].

Recently, ant colony optimization, differential evolution, particle swarm optimization and the neighbourhood algorithms were successfully applied to history match the PUNQ-S3 reservoir [Hajizadeh et al. 2011]. The model was parameterized using 5 layers and 9 homogenous regions per layer. This led to 45 porosity values that were adjusted using the above mentioned population-based algorithms. Horizontal and vertical permeabilities then were obtained using the published deterministic relationship from least square fitting of the well data crossplots [Boss, 1999]. All of the history matching runs contain 3000 models. The detailed parameterization and objective function used for calculating the misfit values can be found in Hajizadeh et al. [2011]. Tables 1-4 present the tuning parameters and the best misfit values obtained in these runs.

Table 1: Algorithm parameters and best misfit obtained for Ant Colony Optimization (ACO_R)

Number of ants	*k*	*q*	*Xi*	Generations	Best Misfit
50	50	0.4	0.7	60	1.83

Table 2: Algorithm parameters and best misfit obtained for Differential Evolution (DE)

Algorithm	N_p	*F*	C_r	Generations	Best Misfit
DE-Rand	50	0.5	0.7	60	1.95
DE-Best	50	0.5	0.5	60	1.45

Table 3: Algorithm parameters and best misfit obtained for Neighbourhood Algorithm (NA)

n_{si}	n_s	n_r	Generations	Best Misfit
50	50	50	60	4.07

Table 4: Algorithm parameters and best misfit obtained for Particle Swarm Optimization (PSO)

Swarm size	Inertial Weight	C_1	C_2	Generations	Best Misfit
50	0.8-0.4	1	2	60	1.51

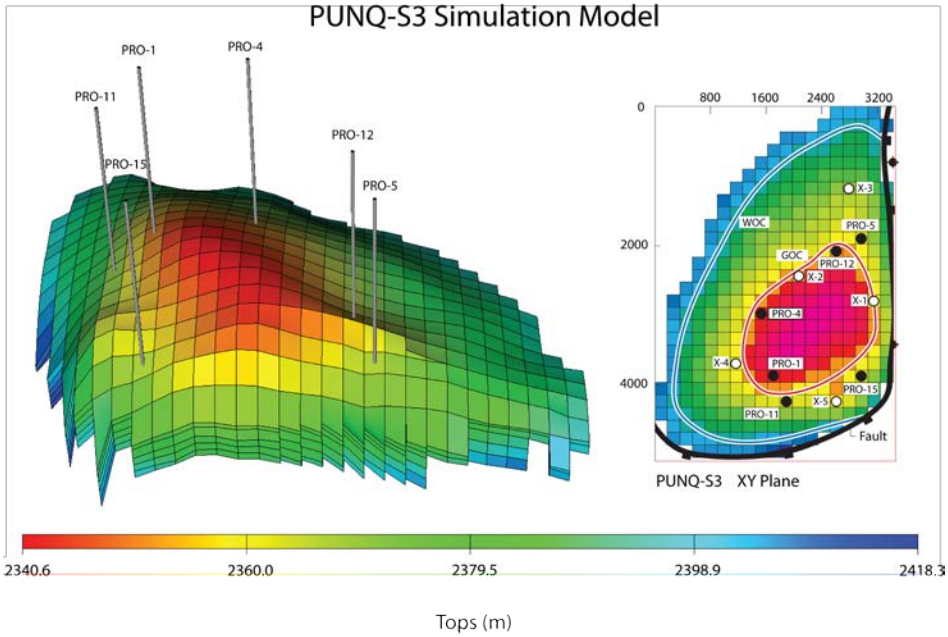

Figure 1: PUNQ-S3 reservoir model with top surface map and well positions

Figure 2 shows the convergence graph for ACO_R, DE, PSO and NA applied for history matching of the PUNQ-S3 reservoir. It plots the best misfit value in each generation vs. the generation number. Each generation of the algorithms used in this work contains 50 members. We can see that DE-Best and PSO have similar trends in convergence, while DE-Best obtains a slightly better final misfit. The NA exhibits a slow convergence with higher misfit values compared to other algorithms. We used extreme exploration setting for NA (n_s/n_r=1) to perform widest search [Sambridge, 1999 a]. Less explorative tunings resulted in larger misfit values, possibly due to over-refinement of local minima.

Although figure 2 and the minimum misfits given in tables 1-4 provide some information about the performance of these algorithms and can be used as a basis for choosing the optimum solutions, some questions still remain open. For example, what is the difference between DE-Best and PSO in this case? While both DE-Best and PSO have a quick convergence and low misfit values, which ensemble should be selected for decision making?

Some users in the history-matching community may think of sorting the results based on misfit values and selecting the top few models for their decision making. If we sort all 3000 models obtained in the above history matching problem based on misfit values and note down top five misfits, we get table 5. Again based on this table, we see that DE-Best and PSO are giving similar misfit values for their best models, while the gap between top misfit values are larger for NA and DE-Rand algorithms. Do the reported numbers in table 5 guarantee that DE-Best and PSO models will give a good prediction for future production and results obtained from NA should be disqualified from being used in the uncertainty quantification study? These questions cannot be addressed using best misfit values and the convergence graphs. In other words, misfit value is not the only dictating criterion in selecting the history matched model(s) for further field development studies.

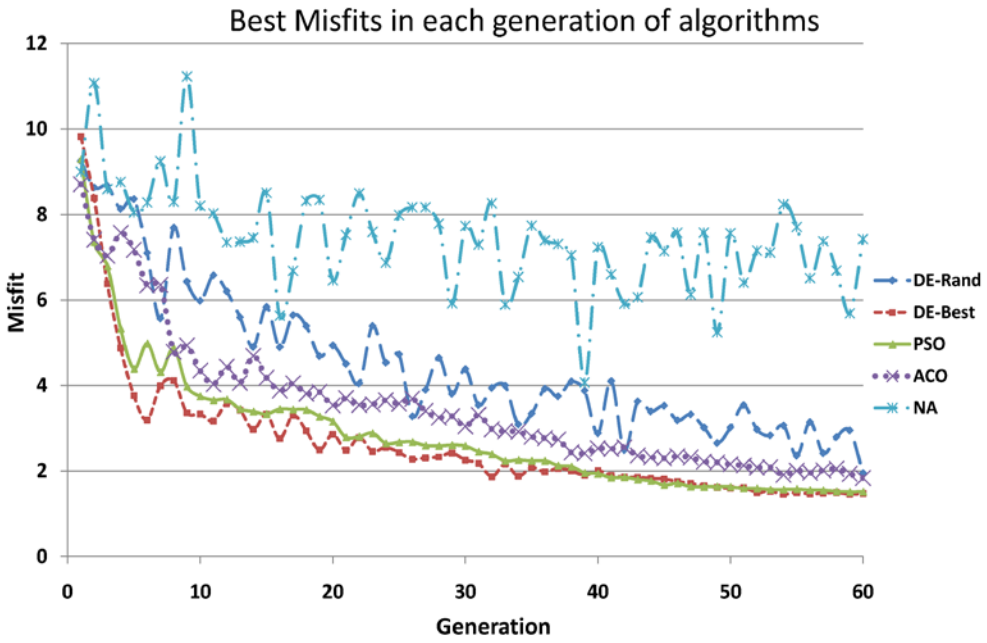

Figure 2: Comparison of convergence speed for different algorithms in history matching of PUNQ-S3 model – [Hajizadeh et al. 2011]

Table 5: Top five misfit values in an ensemble of 3000 history-matched models using various algorithms

Algorithm	Top five misfit values				
ACO_R	1.83	1.91	1.92	1.93	1.96
DE-Rand	1.95	2.35	2.41	2.48	2.65
DE-Best	1.45	1.46	1.46	1.47	1.47
PSO	1.51	1.51	1.52	1.52	1.52
NA	4.07	5.24	5.63	5.68	5.89

One idea to gain more information about the performance of these algorithms is plotting the sampled value vs. the simulation number for the parameters being adjusted in history matching. As there are 45 parameters in the PUNQ-S3 model, plotting 45 separate windows for examining the performance of sampling algorithms for each individual variable is not an appealing idea. This brings the challenge of visualizing the sampling performance in high dimensions which can be addressed using multidimensional projection.

Visualization of Results – Multidimensional Projection

In this section, we present the ensembles of history-matched models projected on a 2D surface. These projections summarize the performance of various population-based sampling algorithms in navigating the 45 dimensional search space in the PUNQ-S3 problem. We deliberately did not include misfit values as a visualization component (color of the points) since the main idea behind the uncertainty quantification method used in this study is that all models (even the ones with high misfit) contain valuable information and contribute to uncertainty quantification [Sambridge, 1999 b]. Instead, we used color as an indication of the iterations of algorithms. This gives an idea about the start and end points of the sampling in time.

In this section, the Euclidian distance is used as a measure of similarity between points. Euclidean distance is a special form of the general Minkowski metric (L_p) which is defined as:

$$L_p(\boldsymbol{x}_a, \boldsymbol{x}_b) = \sum_{i=1}^{d} \left(\left| \boldsymbol{x}_{i,a} - \boldsymbol{x}_{i,b} \right|^p \right)^{1/p} \quad (9)$$

For p=2, we have the Euclidean distance. Figure 3 and 4 present the projections using LSP and ProjClus algorithms and the

Euclidean similarity measure.

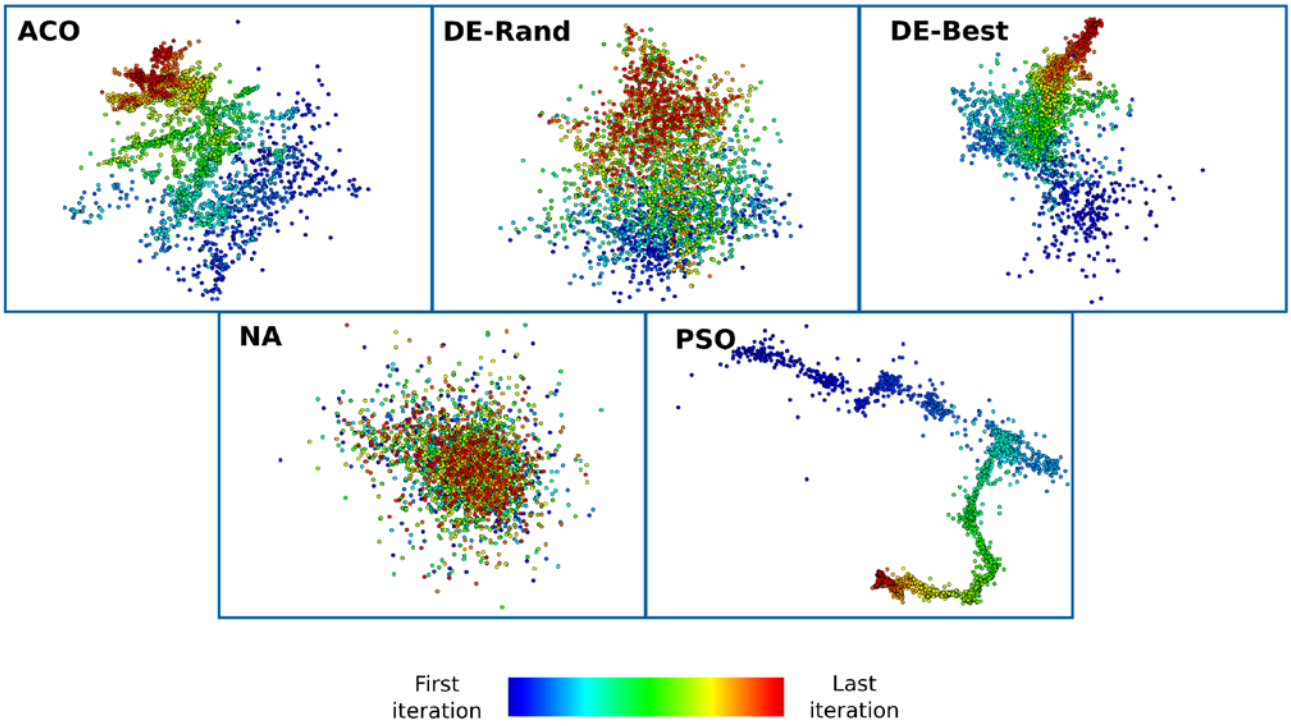

Figure 3: Projection of sampled models using LSP algorithm and Euclidean distance measurement

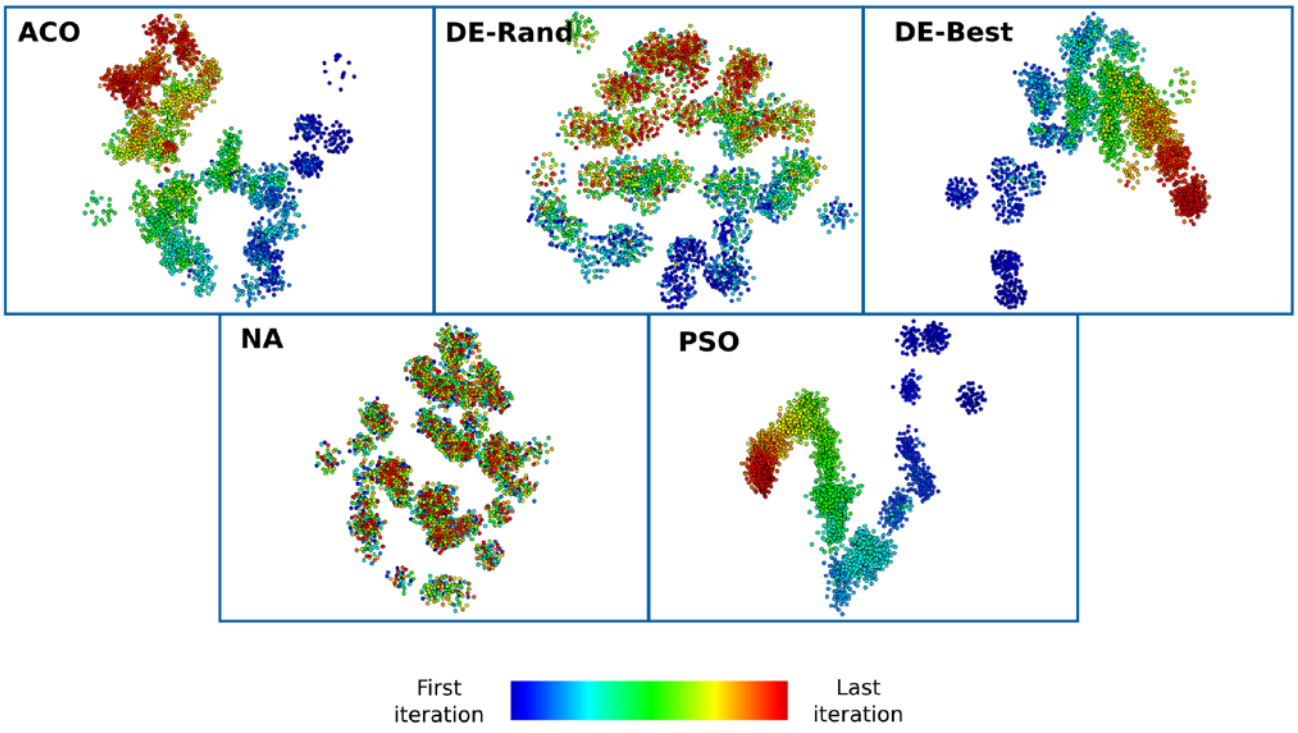

Figure 4: Projection of sampled models using ProjClus algorithm and Euclidean distance measurement

Figure 5 shows the projection results using the PCA algorithm.

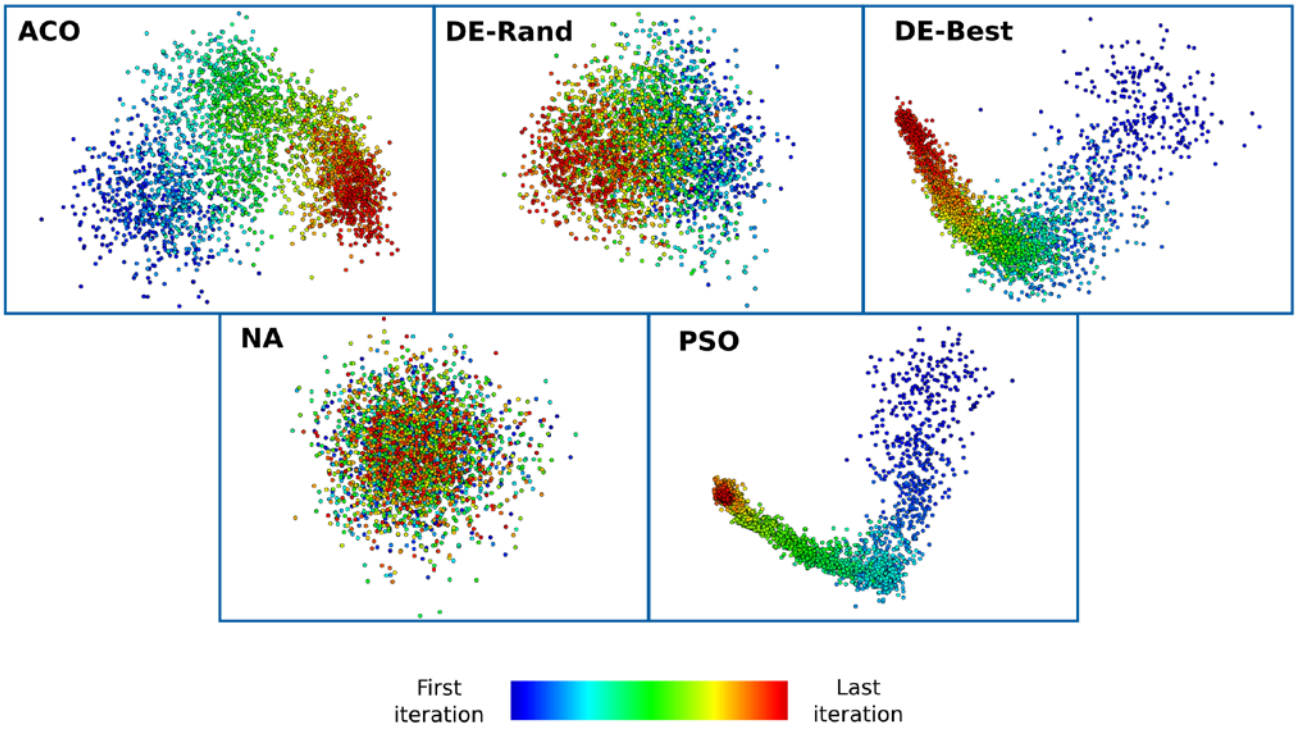

Figure 5: Projection of sampled models using PCA

The projections shown on Figures 3, 4 and 5 provide a totally new insight concerning the performance of population-based sampling algorithms during history matching. Vector selection strategy in differential evolution (DE) is reflected in these projection results. In DE-Rand, the base vector for building the next generation of solutions is selected randomly, while in DE-Best, the solution with the lowest misfit is selected as the base vector. In the projection results we see the difference between the sampling performances of these two strategies of DE. A dense collection of points on the 2D projection indicates convergence of the algorithm towards a specific region of the parameter space in higher dimensions. We can also have this judgment about sampling for other algorithms. While PSO shows a similar behavior to DE-Best, the other three algorithms (DE-Rand, ACO_R and NA) perform a wider search in the 45-dimensional search space. Among the latter three, ACO_R gets more dense points and focuses in specific regions of the search space at the end. DE-Rand and NA demonstrate a very similar pattern in exploring the possible solutions, however in final iterations DE-Rand explores a specific region of the space.

The projection graphs provide a very quick and useful tool to compare various ensembles of history matched models and understand their differences. This can be a valuable tool in selecting the ensemble that better fits in the scope of the project for decision making.

What if we choose another distance measure?

All multidimensional projections techniques use a measure of proximity (similarity) to build their projections. The choice of similarity or distance may have a strong impact on the projection results. In the above section, we chose the widely used Euclidean distance. In this section, we look at two alternate distance measures.

The city block distance or the “Manhattan” metric is another form of the Minkowski metric where p=1 in equation 9. City block is the first distance measure that we are going to use as an alternate to the Euclidean measure in this section. The extended Jaccard is the second similarity measure that we will be investigating. It was introduced by Strehl and Ghosh [2000] and is defined using the following equation:

$$s^{(j)}(x_a, x_b) = \frac{x_a^T x_b}{\|x_a\|_2^2 + \|x_b\|_2^2 + x_a^T x_b} \quad (10)$$

The original Jaccard coefficient measures the ratio of the intersection of the product sets to the union of the product sets for binary features. The extended Jaccard similarity takes the Jaccard measure a step forward and captures a length-dependent measure of similarity for real-valued features.

Few works consider the effect of different measures of similarity on the performance of data exploration, knowledge discovery and projection algorithms. Glazko and Mushegian [2010] studied the performance of various distance measurements in gene expression profiles and concluded that different trends exist in the high dimensional data and different similarity measures highlight different some of these trends. Pereira et al. [2009] performed a study for the similar problem and stated that Euclidean distance has the advantage of not amplifying the noise. Strehl et al. [2000] compared the performance of four popular similarity measures (Euclidean, cosine, Pearson correlation and extended Jaccard) in conjunction with clustering algorithms in high dimensional web-document clustering. They concluded that the Euclidean measurement had the poorest performance, while cosine and extended Jaccard measures were the best measure to capture human categorization behavior. Rady [2011] stated that for face recognition problems, Euclidean distance performs better than the city block measure. Reviewing these literatures, we understand that the choice of similarity measurement very much depends on the application and domain knowledge and no global recommendation can be made.

Figure 6 and 7 show the results of projection for LSP and ProjClus algorithms using the city block distance measurement.

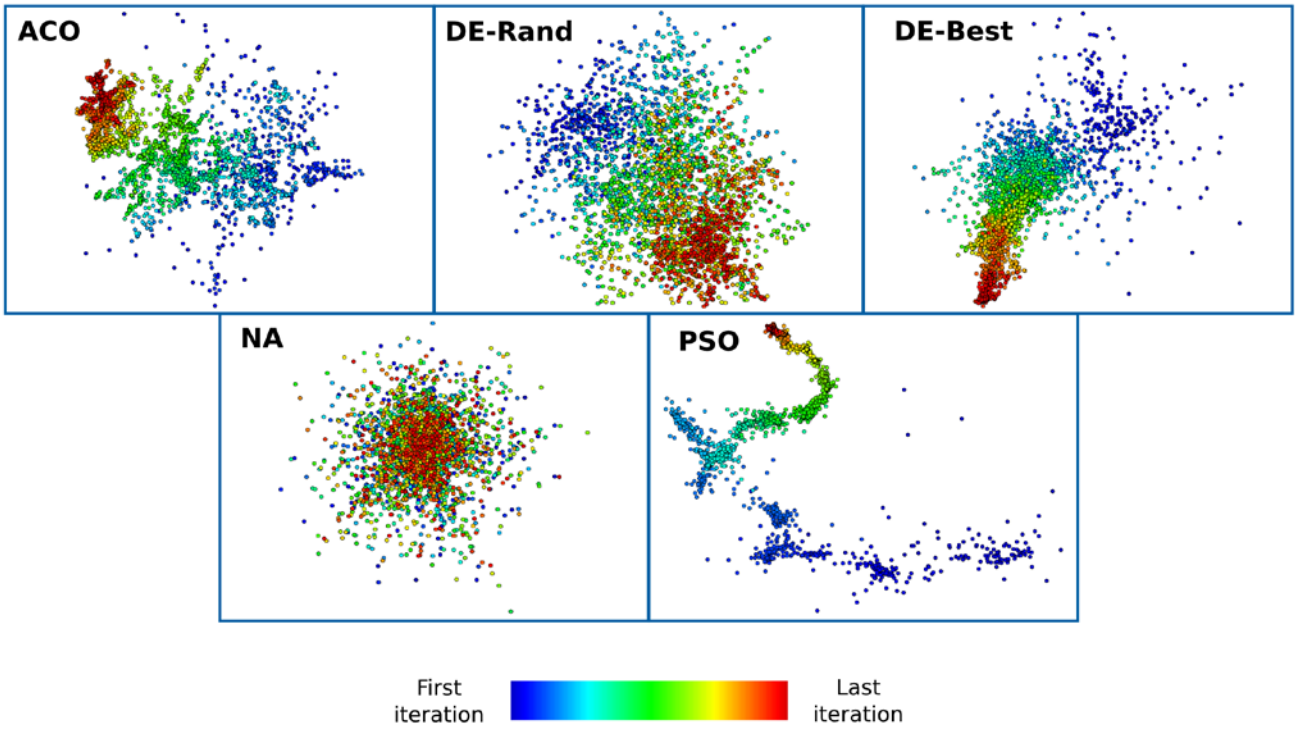

Figure 6: Projection of sampled models using LSP algorithm and city block distance measurement

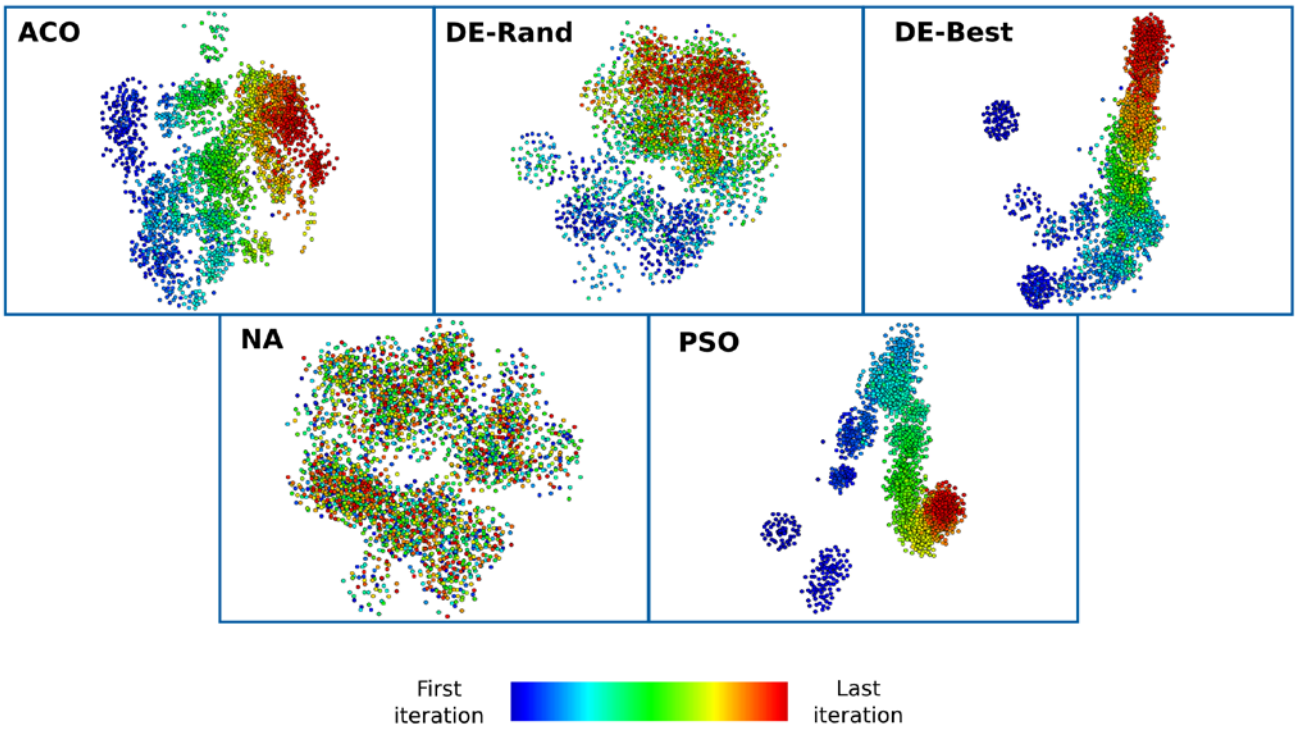

Figure 7: Projection of sampled models using ProjClus algorithm and city block distance measurement

Figures 8 and 9 present the projections using extended Jaccard measurement in LSP and ProjClus algorithms.

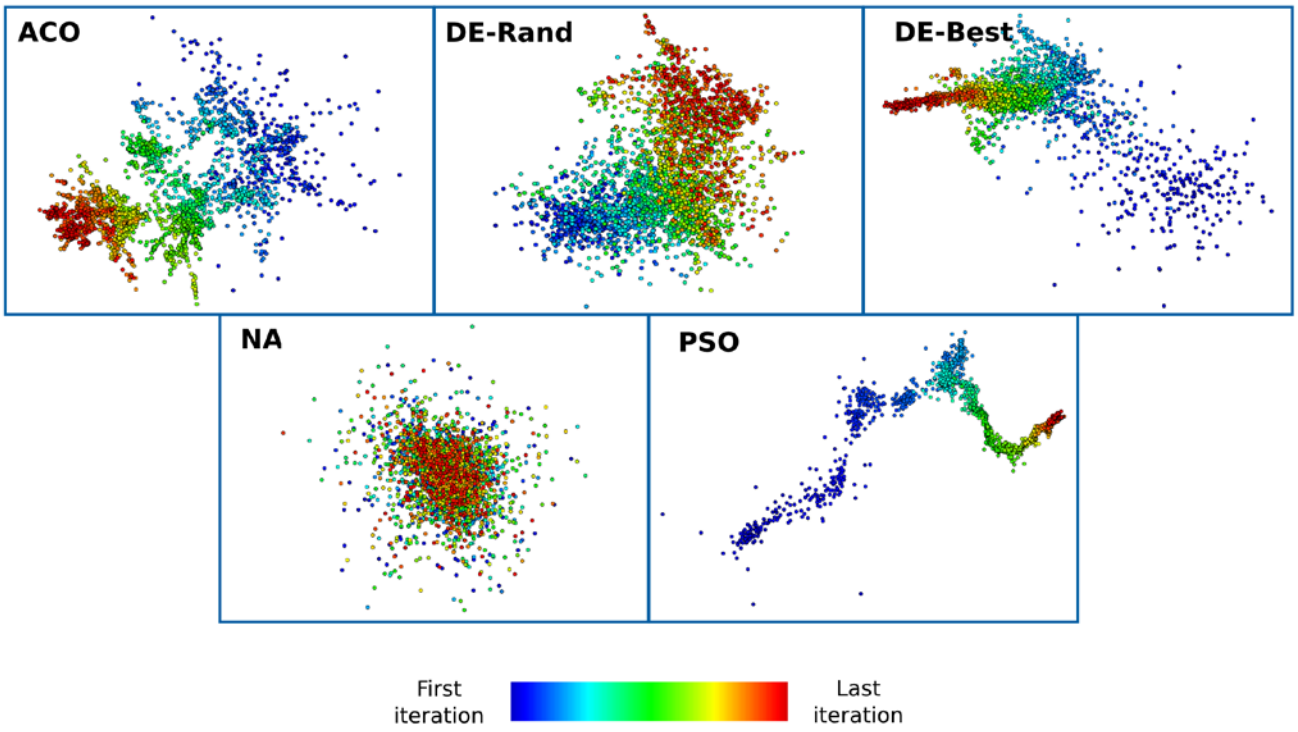

Figure 8: Projection of sampled models using LSP algorithm and extended Jaccard distance measurement

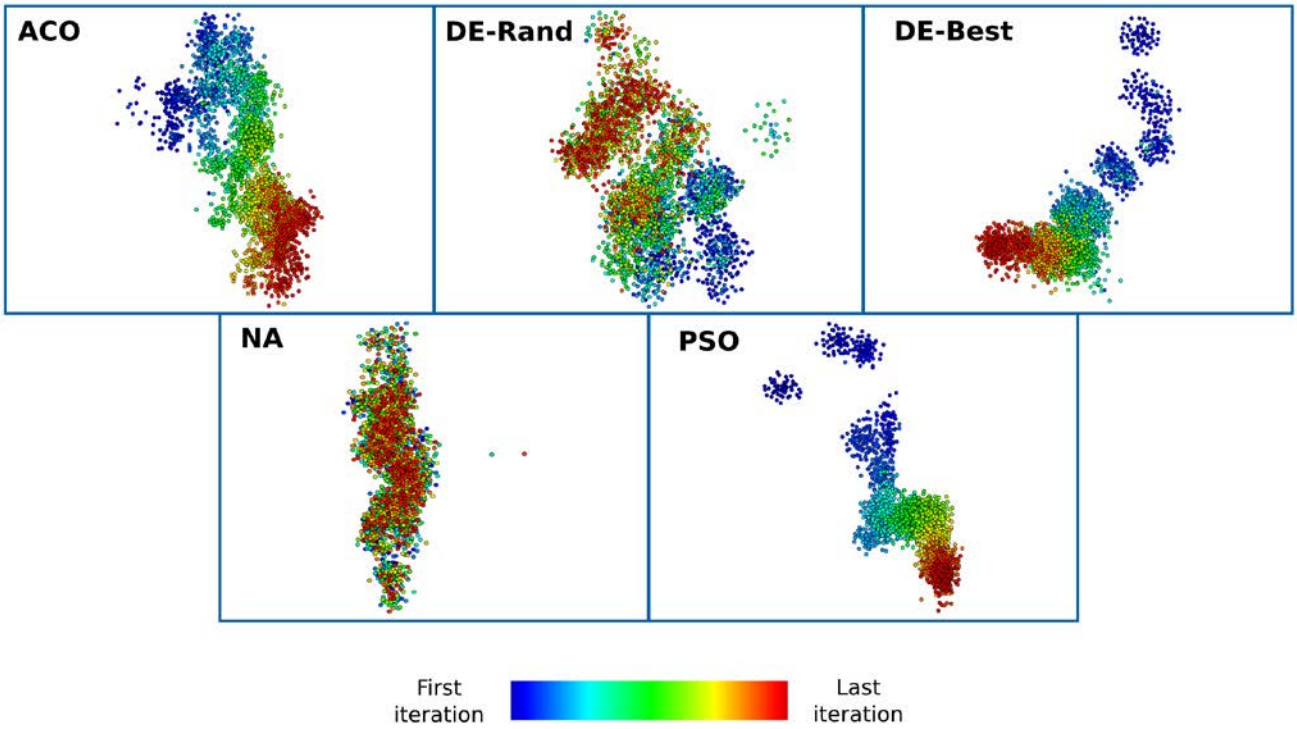

Figure 9: Projection of sampled models using ProjClus algorithm and extended Jaccard distance measurement

The choice of distance measurement between points has some slight impacts on the projections of history-matched models. For example in the ProjClus algorithm, the city block measure (figure 7) makes the clusters appear more dispersed in comparison with the Euclidean distance measure (figure 4). The LSP and ProjClus results tend to be denser using the extended Jaccard distance measure in comparison with both city block and Euclidean measures. This is especially true for the ProjClus algorithm where we can observe very compact clusters in figure 9. Although the choice of distance measure leaves its footprints in the projections, the results we obtain from comparing different history-matched models and their sampling performance are valid for all of the distance measures we have explored in this paper.

Uncertainty and the Multidimensional Projections

After exploring the search space and generating the ensemble of models by different optimization (sampling) algorithms, the next step is to draw inference from the completed ensemble of history-matched models. In a Bayesian framework, the analytical solution of posterior probability requires the integration of the likelihood function over the all possible values of the remaining parameters. In this work, the NA-Bayes (NAB) algorithm [Sambridge, 1999 b] is used for posterior inference. NAB is a Markov chain Monte Carlo (McMC) method which builds an approximation for the real posterior probability distribution (PPD) using a Gibbs sampler. In general, each sampling performed by a McMC method requires evaluation of the objective function at the specific point. The NAB routine requires that forward simulation has been performed for all of the models in ensemble and their (mis)fit to observed data are known. This step has already been performed using various sampling algorithms – in this work ACO_R, DE, PSO and NA.

Before we investigate the relationship between the multidimensional projections and the uncertainty in estimation of the ultimate recovery in our PUNQ-S3 example, we first briefly review the working mechanism of NAB algorithm. Figure 10 summarizes the procedure of the NAB algorithm for a two dimensional problem. The algorithm starts the first step from an arbitrary location (a model in the sampled ensemble) and performs a series of random walks along each parameter axis in turn. For each axis (parameter), a conditional probability distribution function (PDF) is created for the full parameter range (for example the XX' or YY' cut line in figure 10). The probability is determined from the product of the PPD value and the width of the intersection. Each walk is performed on the selected axis by generating a uniform random deviation from the conditional PPD along the axis. After many independent walks starting from different locations, the constructed conditional PDF is believed to be a good approximation to the true posterior distribution. This process can be visualized as several thousand scans of the PPD surface on the parameter axes.

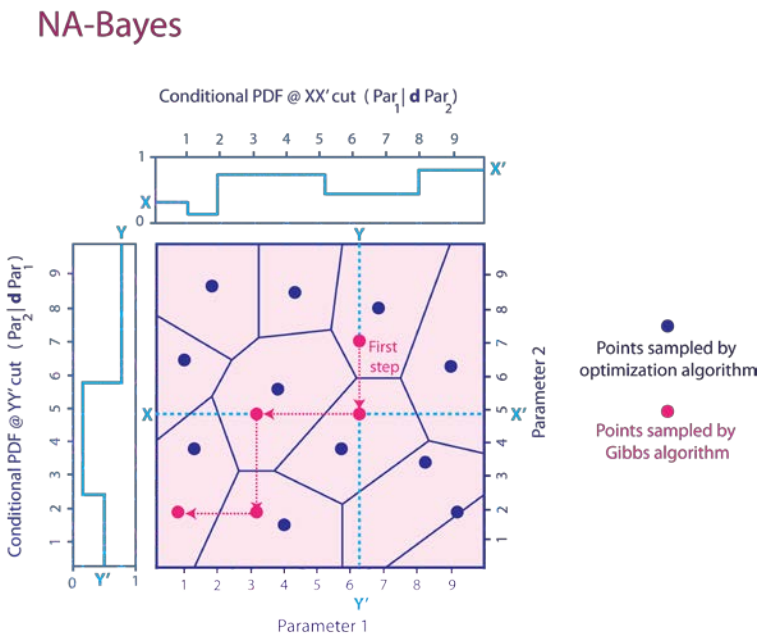

Figure 10: Working mechanism of the NAB algorithm

Reviewing the procedure of the NAB algorithm, we understand that the accuracy of the algorithm depends on the representation of the search space using Voronoi cells. NAB uses Voronoi cells as a surrogate to represent the model space and to interpolate the PPD of unknown points in the search space. This carries an assumption that the misfit value is constant over each Voronoi cell. The interpolation of the misfit surface relaxes the need for running a forward reservoir simulation for posterior sampling. The complexity of the misfit surfaces and the size of samples to represent the search space will affect our prediction and the uncertainty associated with it. The shape and size (volume) of Voronoi cells are determined by distribution of the models obtained using the sampling algorithm. This can be problematic in cases where there is a complex misfit surface (large change of misfit value within short distance) or a limited number of samples (large Voronoi cells).

Figure 11 shows the uncertainty of the predictions obtained after running the NAB algorithm on the ensemble of history-matched models using ACO_R, DE (Rand & Best), PSO and NA.

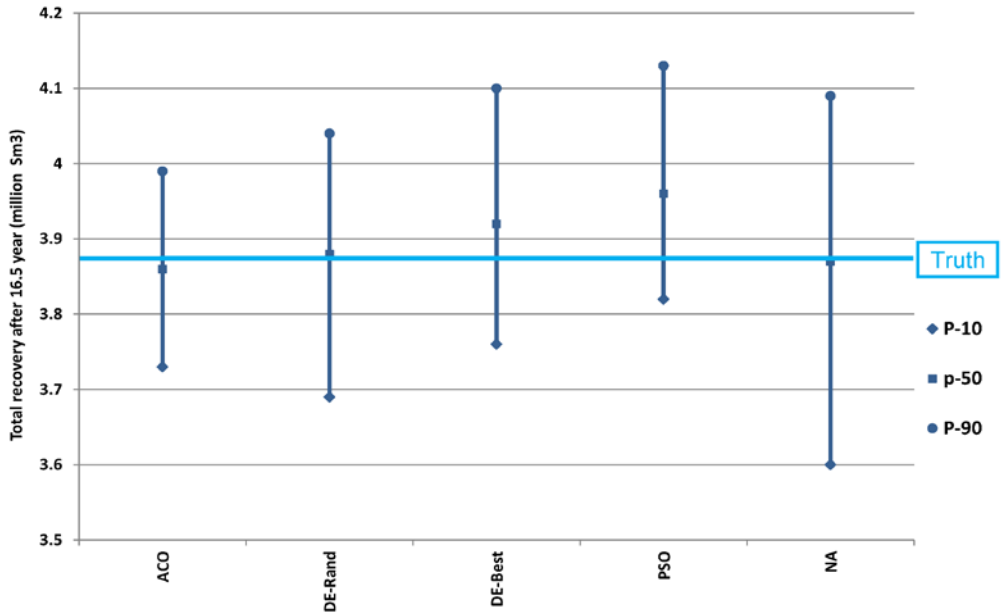

Figure 11: Uncertainty estimates for ACO_R, DE, PSO and NA

The forecast ranges from all algorithms used in this work comfortably cover the truth total production from PUNQ-S3 model. We notice that PSO and DE-Best over-estimate the total oil recovery. DE-Best gives an estimate which is slightly closer to the truth solution in this case. An interesting observation is the range given by NA which had a relatively poor performance during history matching process.

Comparing the projections of sampled models with the uncertainty estimates presented in figure 11, we can see a relationship between these two. PSO and DE-Best quickly converge to a specific region of the search space in the projection figures and this is reflected in their over-estimation of the uncertainty. The sampling performance of DE-Rand and NA are very similar and both cover a wide area (volume) of the search space. Consequently, the uncertainty envelope and P50 values obtained from these two ensembles are similar and close to the truth ultimate recover. We can also draw the same conclusion for ACO_R algorithm with its wide sampling behavior.

The ability of sampling algorithms to give accurate uncertainty estimates is partially linked to the quality of underlying proxy model used for McMC sampling. In our uncertainty quantification framework, the search space is partitioned using Voronoi cells with an assumption that misfit value is constant and equal to misfit of the sample used to generate that cell. Obviously the number and quality of the sampled points used in building the Voronoi cells affect the results of random walks performed by McMC for uncertainty quantification purpose. A quick convergence to a specific region of the search space may result in having large Voronoi cells for other regions with constant misfit surfaces. However there might exist some local minima in those unexplored regions which do not go well with the assumption of constant misfit over that region in performing a random walk.

Although not backed by solid experiments in this study, the above concept should also be true for other proxy modeling techniques used in uncertainty quantification. The power of a proxy model depends on the samples used to build it. Having a poor quality proxy model in some regions of the search space may result in unrealistic estimates of production (or other target values) in uncertainty quantification.

In agreement with a study performed by Tavasoli et al. [2004] that showed a good history-matched model does not necessarily lead to a good prediction, we demonstrate an example (NA) where a not-so-good model in the history matching phase gives a reasonable forecast envelope due to its wide sampling of the search space. This study suggests that in the history matching context, exploration of search space is more important that the exploitation phase. On the other hand, size of model and available resources to run simulations play an important role in selecting the maximum number of simulations in a history matching study.

While this study shows the importance of exploring the search space, it does not suggest a pure random search to cover a large portion of search space as an effective strategy in history matching. Wan and Igusa [2003] discussed the need for greater accuracy in regions of the search space corresponding to low misfit values and the benefits of adaptive sampling methods to satisfy this purpose. This study once again stresses the importance of exploration vs. exploitation in assisted history matching using population-based sampling algorithms.

Conclusions

This paper provides a roadmap to incorporation of multidimensional projections as a part of assisted history matching frameworks. These tools can be utilized to check the performance of evolutionary sampling algorithms during/after history matching. The multidimensional projection allows a quick comparison between ensembles of history matched models using different stochastic population-based methods and/or different tuning parameters of these algorithms. These plots can be used together with the misfit convergence graphs in history matching to gain a better understanding of the sampling process.

The projections can also help in deciding the right amount of exploration vs. exploitation in assisted history matching frameworks. The choice of convergence speed vs. sampling coverage is affected by the goals of project and the available computer resources. However this study suggests that a more exploratory setting for population-based algorithms in history matching is favorable. This is tied with the uncertainty quantification step where we can obtain a more reliable proxy tool to run a Monte Carlo job.

The choice of distance measurement used to check the similarity of sampled points has a slight impact on the projection results. This does not render the conclusions drawn from comparing various ensembles in this work invalid. The comparison between projection schemes and the distance measure in this work is mainly visual. We will keep working on bringing a more formal framework for comparing the performance of projection algorithms that incorporates the measures for computational efficiency, quality of uncertainty estimation and behavior in projecting noisy data. These results will be useful

in designing better assisted history matching workflows.

Acknowledgments

This research was supported by the NSERC/Alberta Innovates Technology Futures (AITF)/Foundation CMG Industrial Research Chair in Scalable Reservoir Visualization.

References

Abdollahzadeh, A., Reynolds, A., Christie, M., Corne, D., Williams, G, Davies, B [2011] Estimation of Distribution Algorithms Applied to History Matching, SPE 141161, SPE Reservoir Simulation Symposium, The Woodlands, Texas, USA, 21-23 February

Bengtsson, T., Bickel, P., Li, B [2008] Curse-of-Dimensionality Revisited: Collapse of the Particle Filter in Very Large Scale Systems, Probability and Statistics: Essays in Honor of David A. Freedman, Institute of Mathematical Statistics, Volume 2, 316-334

Boss, C [1999] Production Forecasting with UNcertainty Quantification, Netherlands Institute of Applied Geoscience, TNO

Buja, A., Cook, D., Hofmann, H., Lawrence, M., Lee, E-K., Swayne, D., Wickham, H [2009] Statistical Inference for Exploratory Data Analysis and Model Diagnostics, Philosophical Transactions of The Royal Society, A, 4361-4382

Christie, M., MacBeth, C., Subbey, S [2002] Multiple History-Matched Models for Teal South, The Leading Edge, Volume 21, Number 3, 286-289

Faloutsos, C., Lin, K [1995] Fastmap: A Fast Algorithm for Indexing, Data Mining and Visualization of Traditional and Multimedia Databases, ACM SIGMOD International Conference on Management of Data, San Jose, CA, USA

Floris, F.J.T., Bush, M.D., Cuypers, M., Roggero, F., Syversveen, A-R [2001] Methods for Quantifying the Uncertainty of Production Forecasts, Petroleum Geoscience, Volume 7, 87-96

Gao, G., Li, G., Reynolds, A.C [2007] A Stochastic Optimization Algorithm for Automatic History Matching, SPE Journal, Volume 12, Number 2, 196-208

Glazko, G., Mushegian, A [2010] Measuring Gene Expression Divergence: The Distance to Keep, Biology Direct, 5, 51

Hajizadeh, Y., Christie, M., Demyanov, V [2009] Ant Colony Optimization for History Matching, SPE 121193, EUROPEC/EAGE Conference and Exhibition, Amsterdam, The Netherlands, 8-11 June

Hajizadeh, Y., Christie, M., Demyanov, V [2010] History Matching with Differential Evolution; A look at New Search Strategies, SPE 130253, EUROPEC/EAGE Conference and Exhibition, Barcelona, Spain, 14-17 June

Hajizadeh, Y., Demyanov, V., Mohamed, L., Christie, M [2011] Comparison of Evolutionary and Swarm Intelligence Methods for History Matching and Uncertainty Quantification in Petroleum Reservoir Models, In Intelligent Computational Optimization in Engineering, Keoppen, M., Schaefer, G., Abraham, A (Eds.) Studies in Computational Intelligence, Springer, Volume 366, 209-240

Hotelling, H [1933] Analysis of a Complex of Statistical Variables into Components, Journal of Educational Psychology, 24, 417-441

Jeong, D.H., Ziemkiewicz, C., Fisher, B., Ribarsky, W., Chang, R [2009] iPCA: An Interactive System for PCA-based Visual Analytics, Eurographics/IEEE-VGTC Symposium on Visualization, Volume 28, Number 3, 767-774

Manceau, E., Mezghani, M., Zabala, I., Roggero, F [2001] Combination of Experimental Design and Joint Modeling Methods for Quantifying the Risk Associated with Deterministic and Stochastic Uncertainties - An Integrated Test Study, SPE 71620, Annual Technical Conference and Exhibition, New Orleans, Louisiana, USA, 30 September-3 October

Mantica, S., Cominelli, A., Mantica, G. [2002] Combining Global and Local Optimization Techniques for Automatic History Matching Production and Seismic Data, SPE 78353, SPE Journal, Volume 7, Number 2, 123-130

Mohamed, L., Christie, M., Demyanov, V [2010] Reservoir Model History Matching with Particle Swarms, Variants Study, SPE 129152, SPE Oil and Gas India Conference and Exhibition, Mumbai, India, 20-22 January

Muller, W., Nocke, T., Schumann, H [2006] Enhancing the Visualization Process with Principle Component Analysis to Support the Exploration of Trends, APVis, Australian Computer Society, Inc, 121-130

Paulovich, F.V., Minghim, R [2006] Text Map Explorer: A Tool to Create and Explore Document Maps. In Proceedings of 10th IEEE Information Visualization International Conference (IV'06), London, UK

Paulovich, F.V., Nonato, L.G., Minghim, R., Levkowitz, H [2006] Visual Mapping of Text Collections through a Fast High Precision Projection Technique, In Proceedings of 10th IEEE Information Visualization International Conference (IV'06), London, UK

Paulovich, F.V., Oliveira, M.C.F., Minghim, R [2007] The Projection Explorer: A Flexible Tool for Projection-based Multidimensional Visualization, Brazilian Symposium on Computer Graphics and Image Processing, SIBGRAPI, Minas Gerais, 7-10 October, PEx tool publicly available at http://infoserver.lcad.icmc.usp.br/infovis2/PEx

Pereira, V., Waxman, D., Eyre-Walker, A [2009] A Problem with the Correlation Coefficient as a Measure of Gene Expression Divergence, Genetics, Volume 183, Number 4, 1597-1600

PUNQ-S3 Model, Department of Earth Science and Engineering, Imperial College London, http://www3.imperial.ac.uk/earthscienceandengineering/research/perm/punq-s3model , Last Accessed December 2011

Rady, H [2011] Face Recognition using Principle Component Analysis with Different Distance Classifiers, IJCSNS International Journal of Computer Science and Network Security, Volume 11, Number 10, 134-144

Romero, C., Carter, J., Zimmerman, R., Gringarten, A [2000] Improved Reservoir Characterization Through Evolutionary Computation, SPE 62942, SPE Annual Technical Conference and Exhibition, Dallas, Texas, USA, 1-4 October

Santos, S., Brodlie, K [2004] Gaining Understanding of Multivariate and Multidimensional Data Through Visualization, Computer and Graphics, 28, 311-325

Sambridge, M [1999 a] Geophysical Inversion with a Neighbourhood Algorithm - I Searching a Parameter Space, Geophysics Journal Int, 138, 479-494

Sambridge, M [1999 b] Geophysical Inversion with a Neighbourhood Algorithm - II Appraising the Ensemble, Geophysics Journal Int, 138, 727-745

Schulze-Riegert, R., Axmann, J., Haase, O., Rian, D., You, Y [2001] Optimization Methods for History Matching of Complex Reservoirs, SPE 66393, Reservoir Simulation Symposium, Houston, Texas, USA,11-14 February

Strehl, A., Ghosh, J [2000] Value-based Customer Grouping from Large Retail Data-sets, SPIE Conference on Data Mining and Knowledge Discovery, Orlando, volume 1057, 33-42

Strehl, A., Ghosh, J., Mooney, R [2000] Impact of Similarity Measures on Web Page Clustering, In Proceedings of the Workshop of Artificial Intelligence for Web Search, Austin, USA, 58-64

Tavasolli, Z., Carter, J. N., King, P [2004] Errors in History Matching, SPE 96883, SPE Journal, Volume 9, Number 3, 352-361

Wan, Z., Igusa, T [2003] Adaptive Sampling for Optimization under Uncertainty, Proceedings of the Fourth International Symposium on Uncertainty Modeling and Analysis (ISUMA), IEEE, 423-428

Yang, J., Ward, M.O., Rundensteiner, E.A., Huang, S [2003] Visual Hierarchical Dimension Reduction for Exploration of High Dimensional Datasets, Joint IEEE/EG Symposium on Visualization, VisSym, Grenoble, France, 19-28